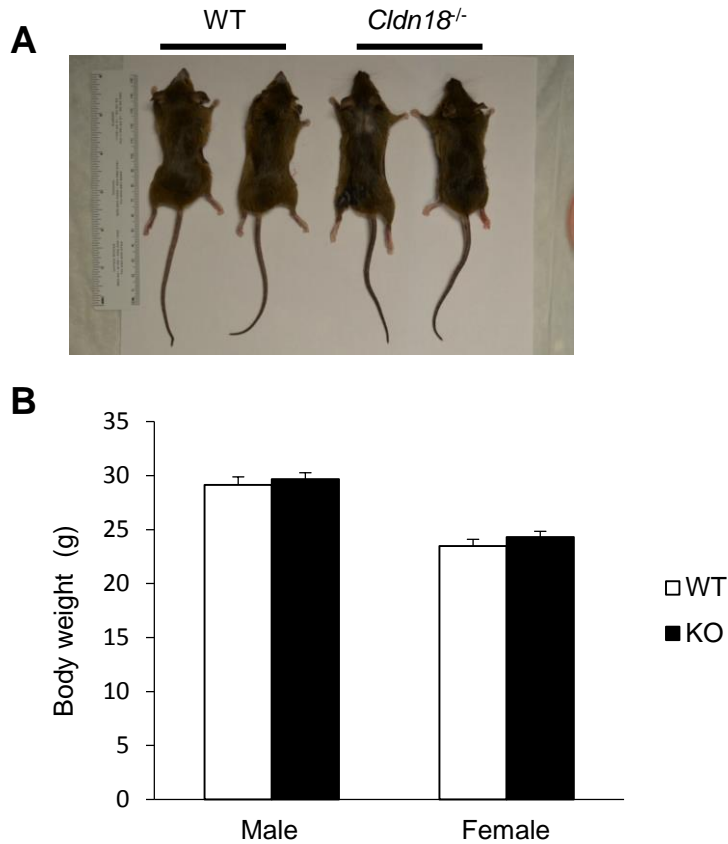
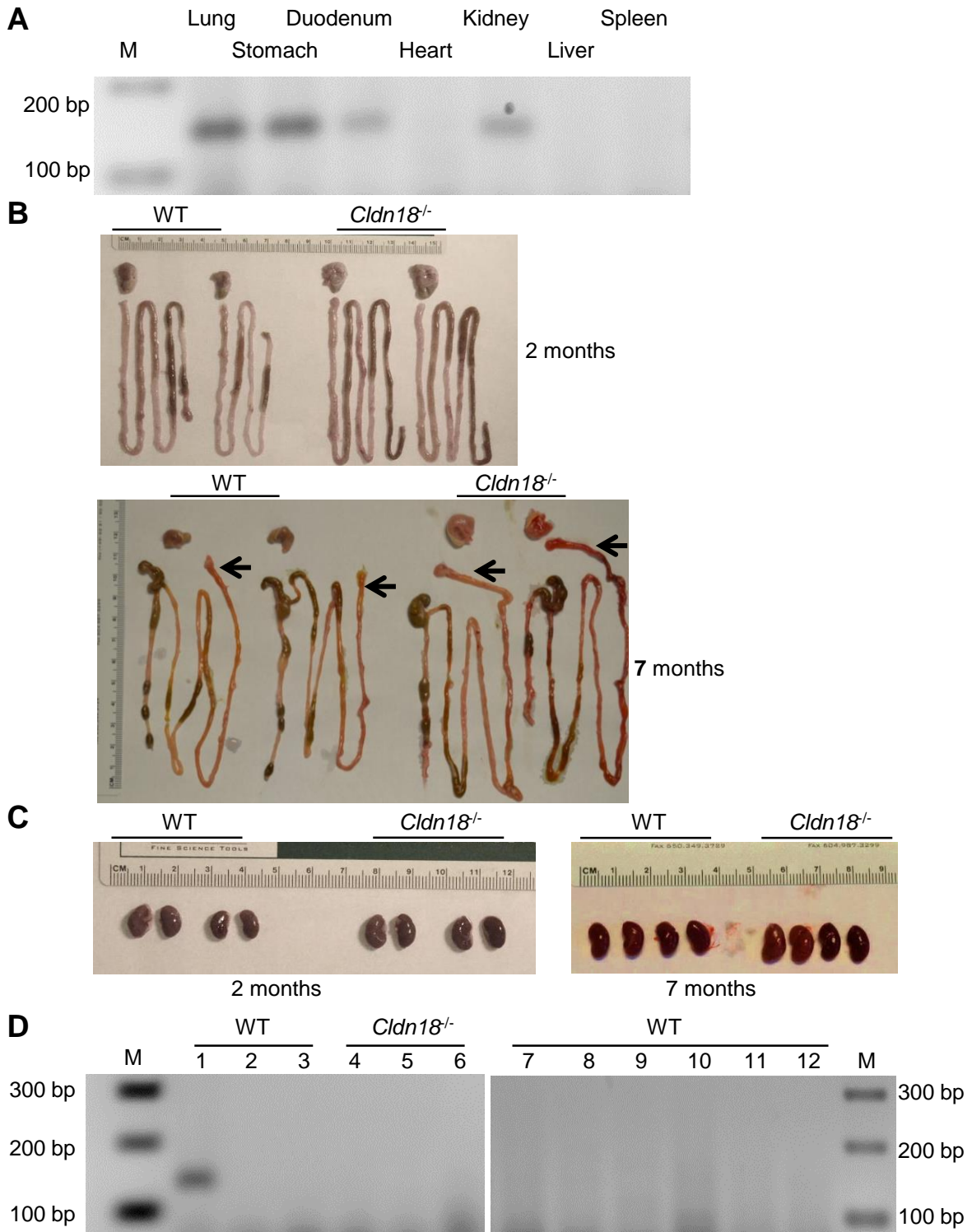


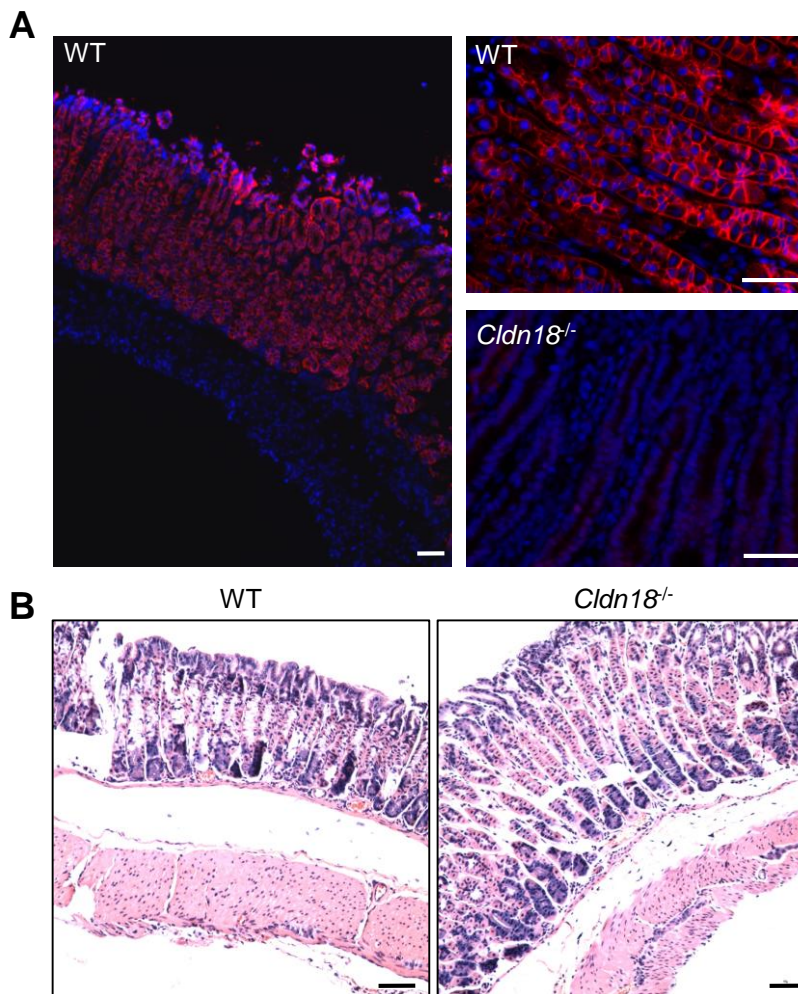
Supplemental Figure 1. Increased cellularity and mean linear intercept in lungs of *Cldn18*^{-/-} mice. (A) Hematoxylin and eosin staining of whole lung sections from WT and *Cldn18*^{-/-} mice at E18, 1 week and 2 and 6 months shows increased cellularity and enlarged alveolar airspaces. Scale bar: 50 μm. **(B)** Increased mean linear intercept (MLI) in lungs of *Cldn18*^{-/-} mice (WT 37.8 ± 1.8 μm and *Cldn18*^{-/-} 51.0 ± 1.3 μm) at 1 month of age. n = 4. Unpaired 2-tailed t-test. *, *P* < 0.05. Bar graphs represent mean ± SEM for **B**.



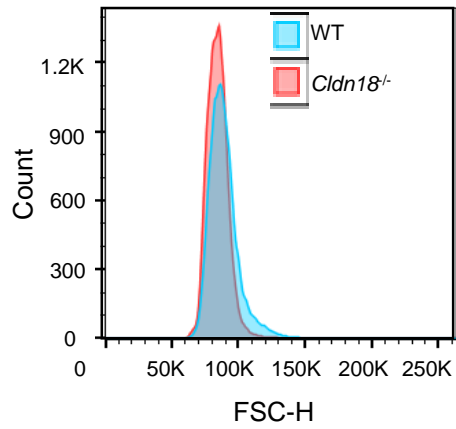
Supplemental Figure 2. Unchanged size and body weight of *Cldn18^{-/-}* mice. (A) WT and *Cldn18^{-/-}* mice are of similar size at age 7 months. **(B)** Weight of WT (29.1 ± 0.7 g (male) and 23.5 ± 0.6 g (female)) and *Cldn18^{-/-}* (29.7 ± 0.6 g (male) and 24.3 ± 0.5 g (female)) mice is similar at ~7 months of age. n ≥ 6. Two-way ANOVA with Bonferroni's correction. Bar graphs represent mean ± SEM for **B**.



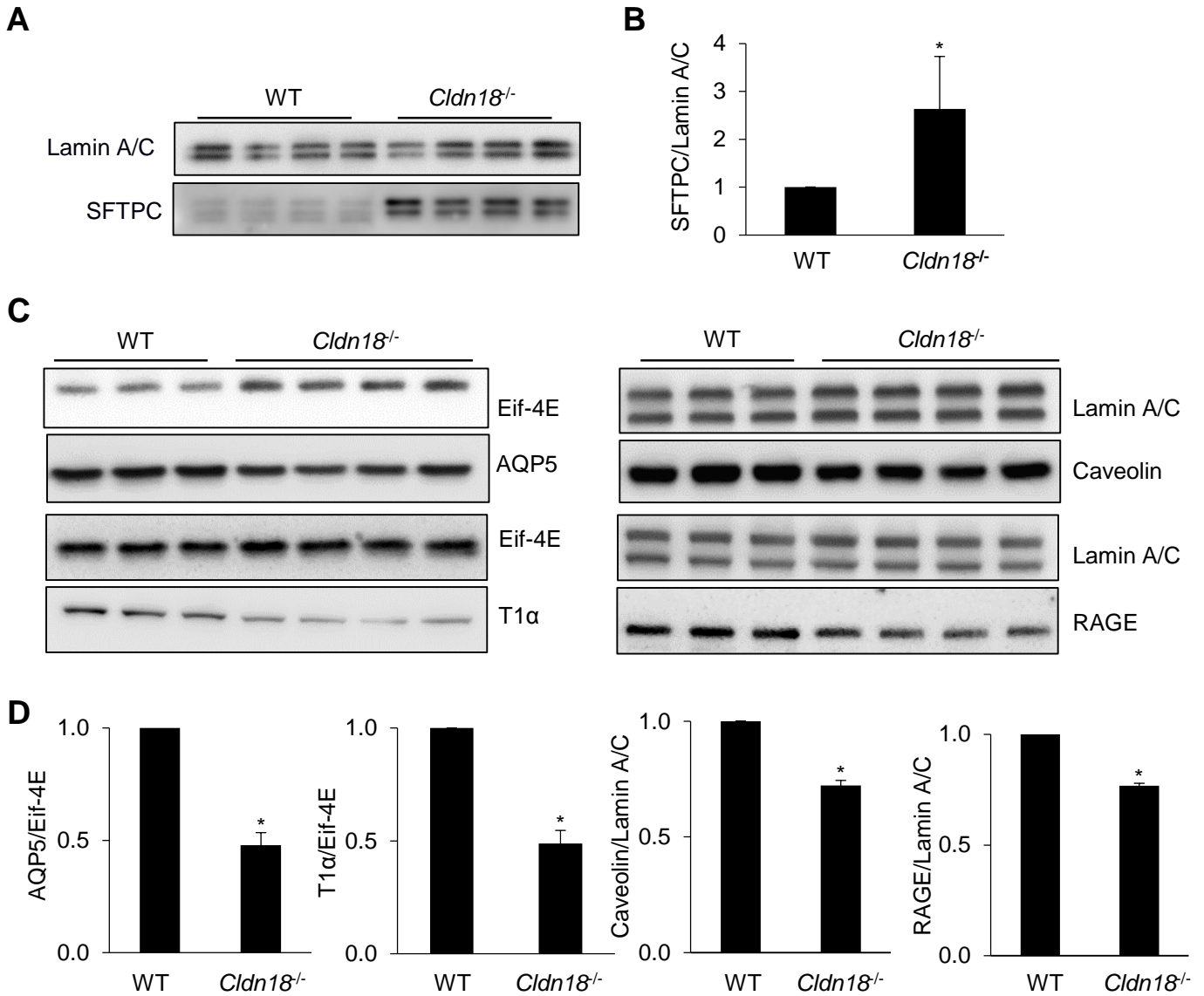
Supplemental Figure 3. Expression of *Cldn18* in different organs. (A) RT-PCR shows that lung, stomach, duodenum and kidney express *Cldn18* while other organs (heart, liver and spleen) do not. Stomach (B) and kidney (C) of *Cldn18*^{-/-} mice at age 2 and 7 months are visibly larger than those of WT mice. Duodenum (B) of *Cldn18*^{-/-} mice is visibly larger than that of WT mice at age 7 months (arrow). (D) RT-PCR shows that trachea, esophagus, brain, intestine, colon, uterus and muscle do not express *Cldn18*, and *Cldn18* is expressed in WT but not *Cldn18*^{-/-} lung (1 and 4: lung; 2 and 5: trachea; 3 and 6: esophagus; 7: brain; 8: trachea; 9: intestine; 10: colon; 11: uterus; 12: muscle; M: marker).



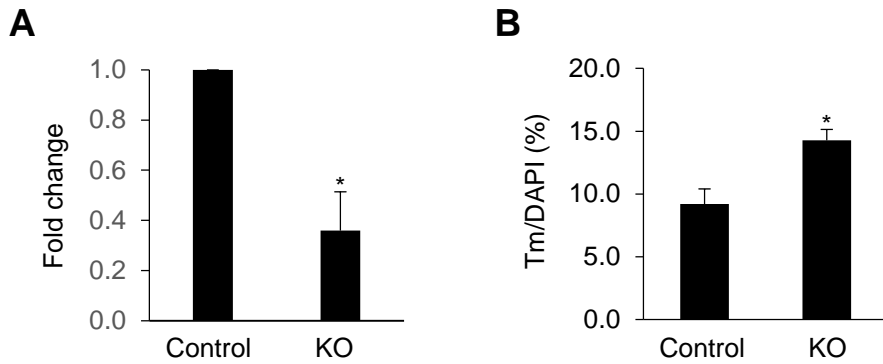
Supplemental Figure 4. Increased gastric mucosal thickness and expansion of proliferative zone in *Cldn18^{-/-}* mice. (A) Immunofluorescence shows CLDN18 (red) expression in stomach of WT but not *Cldn18^{-/-}* mice. DAPI (blue) is the nuclear counterstain. Scale bar: 50 μ m. **(B)** Hematoxylin and eosin staining shows increased gastric mucosal thickness in *Cldn18^{-/-}* compared to WT mice. Scale bar: 50 μ m.



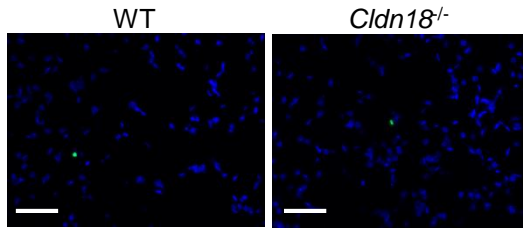
Supplemental Figure 5. Unchanged type II (AT2) cell size in *Cldn18*^{-/-} lungs. Representative flow cytometric analysis reveals no difference in cell size between WT and *Cldn18*^{-/-} AT2 cells. n = 3.



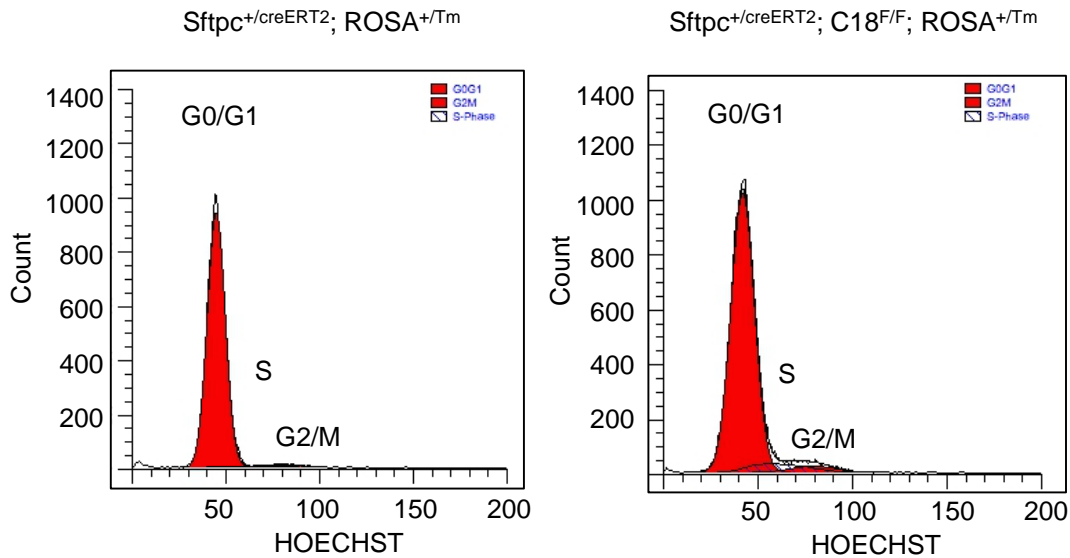
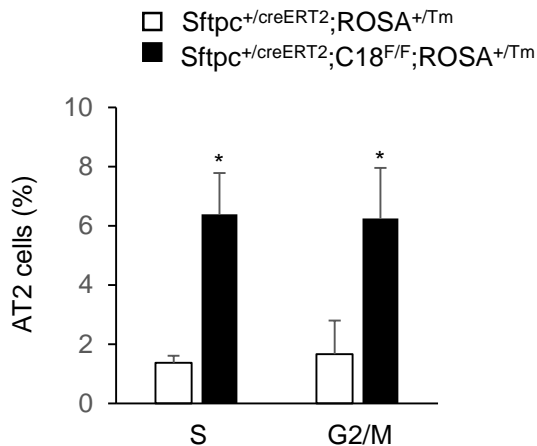
Supplemental Figure 6. Increased expression of type II (AT2) and decreased expression of type I (AT1) cell markers in lung of *Cldn18*^{-/-} mice. (A, B) Whole lung lysates show significantly higher levels of SFTPC in *Cldn18*^{-/-} compared to WT mice. $n = 4$. Z-test. *, $P < 0.05$. Western analysis (C) and quantification (D) in whole lung lysates show significantly decreased expression of AQP5, T1 α , caveolin-1 and RAGE in *Cldn18*^{-/-} compared to WT mice. $n \geq 3$. Z-test. *, $P < 0.05$. Bar graphs represent mean \pm SEM for B and D.



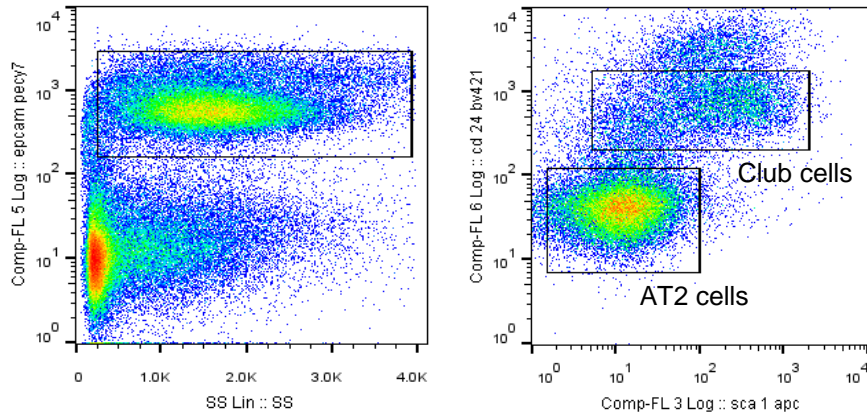
Supplemental Figure 7. Increased type II (AT2) cell number in AT2 cell-specific *Cldn18* KO mice. (A) *Cldn18* mRNA is decreased in isolated AT2 cells one week after administration of tamoxifen (Tmx) intraperitoneally for 2 days at a dose of 100 mg/kg to *Sftpc*^{+/*creERT2*};*C18*^{F/F};*ROSA*^{+/*Tm*} mice (KO) compared to *Sftpc*^{+/*creERT2*};*ROSA*^{+/*Tm*} mice (control). n = 3. Z-test. *, *P* <0.05. (B). Tomato⁺ (Tm⁺) AT2 cells are increased in *Sftpc*^{+/*creERT2*};*C18*^{F/F};*ROSA*^{+/*Tm*} compared to *Sftpc*^{+/*creERT2*};*ROSA*^{+/*Tm*} mice ~ 5 months following Tmx injection at the age of 1-2 months. n = 5. Z-test. *, *P* <0.05. Bar graphs represent mean ± SEM for **A** and **B**.



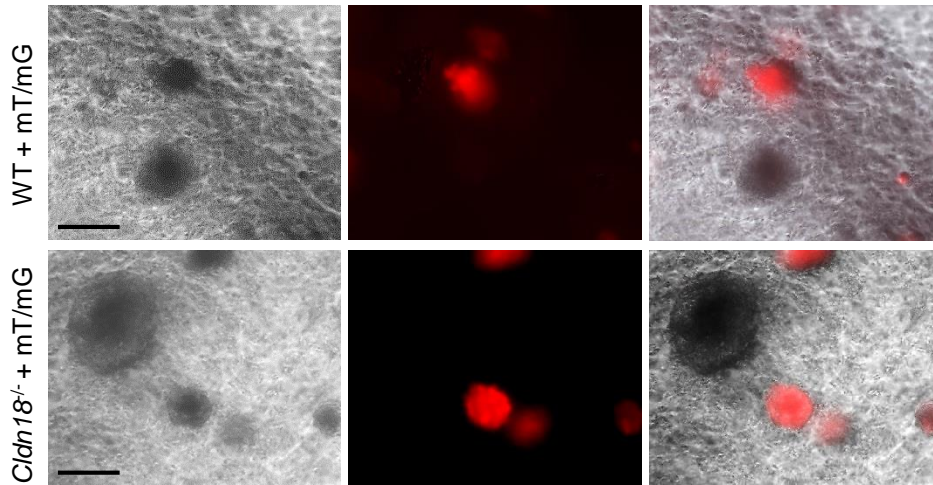
Supplemental Figure 8. Apoptosis in lungs of *Cldn18*^{-/-} mice. Representative TUNEL assay shows similarly low numbers of apoptotic cells (green) in distal lung of WT and *Cldn18*^{-/-} mice. n=3 mice for each genotype. Scale bar: 50 μ m.

A**B**

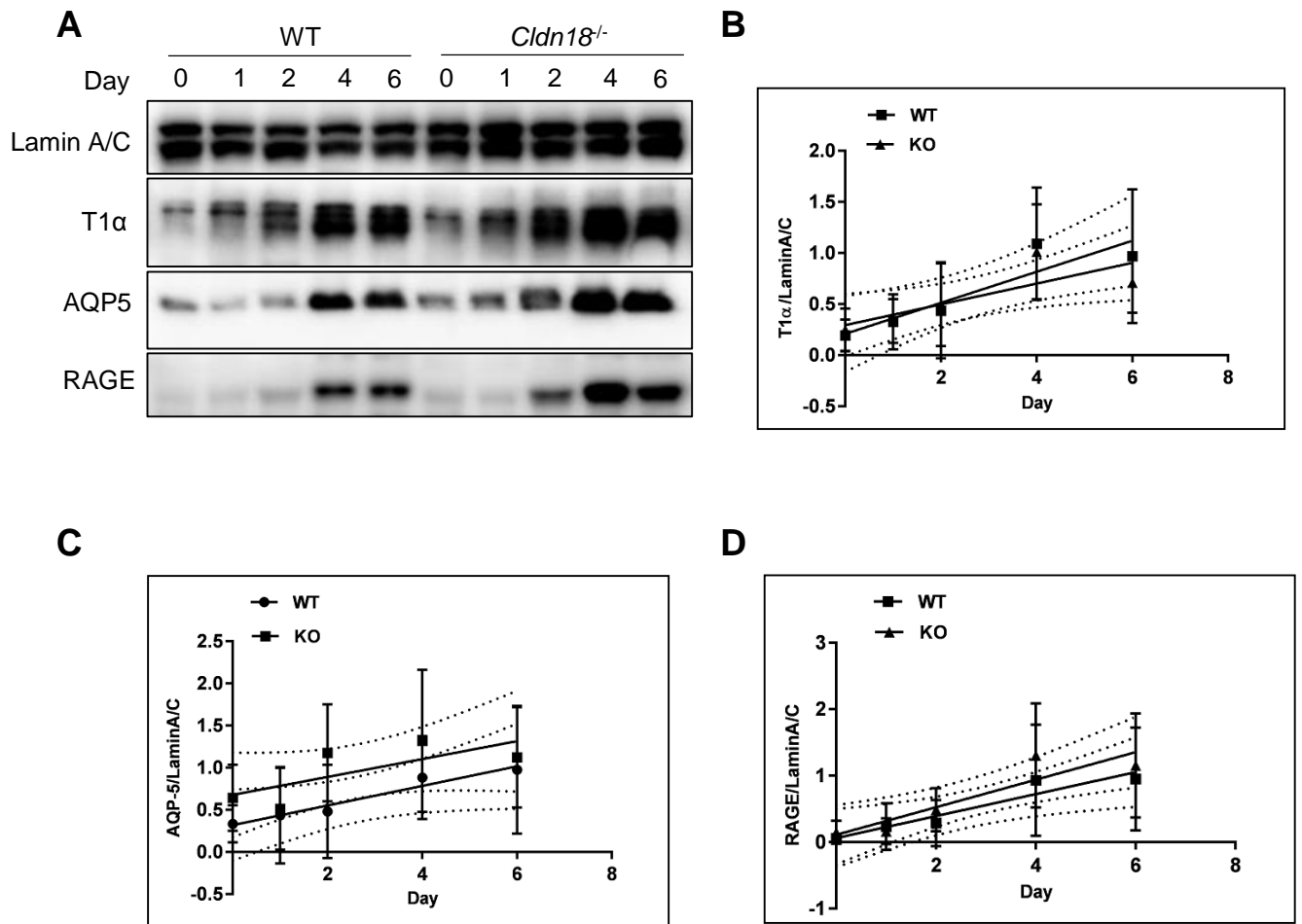
Supplemental Figure 9. Increased type II (AT2) cell proliferation in AT2 cell-specific *Cldn18* KO mice. Representative flow cytometry (A) and quantitation (B) show a greater percentage of AT2 cells in S and G2/M phase in *Sftpc*^{+/creERT2}; *C18F/F*; *ROSA*^{+/Tm} compared to control *Sftpc*^{+/creERT2}; *ROSA*^{+/Tm} mice (1-5 months following Tmx injection at the age of 3-4 months). *n* = 4 mice of each genotype. Two-way ANOVA. *, vs. control mice, *P* < 0.05. Bar graphs represent mean ± SEM for B.



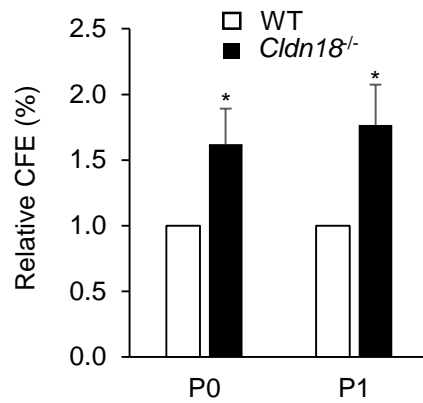
Supplemental Figure 10. Fluorescence activated cell sorting of type II (AT2) cells from WT mice. AT2 cells (EpCAM^{Hi}/CD45⁻CD34⁻CD31⁻CD24⁻SCA1⁻) were sorted from WT mouse lungs. Gates are shown for AT2 and club cells.



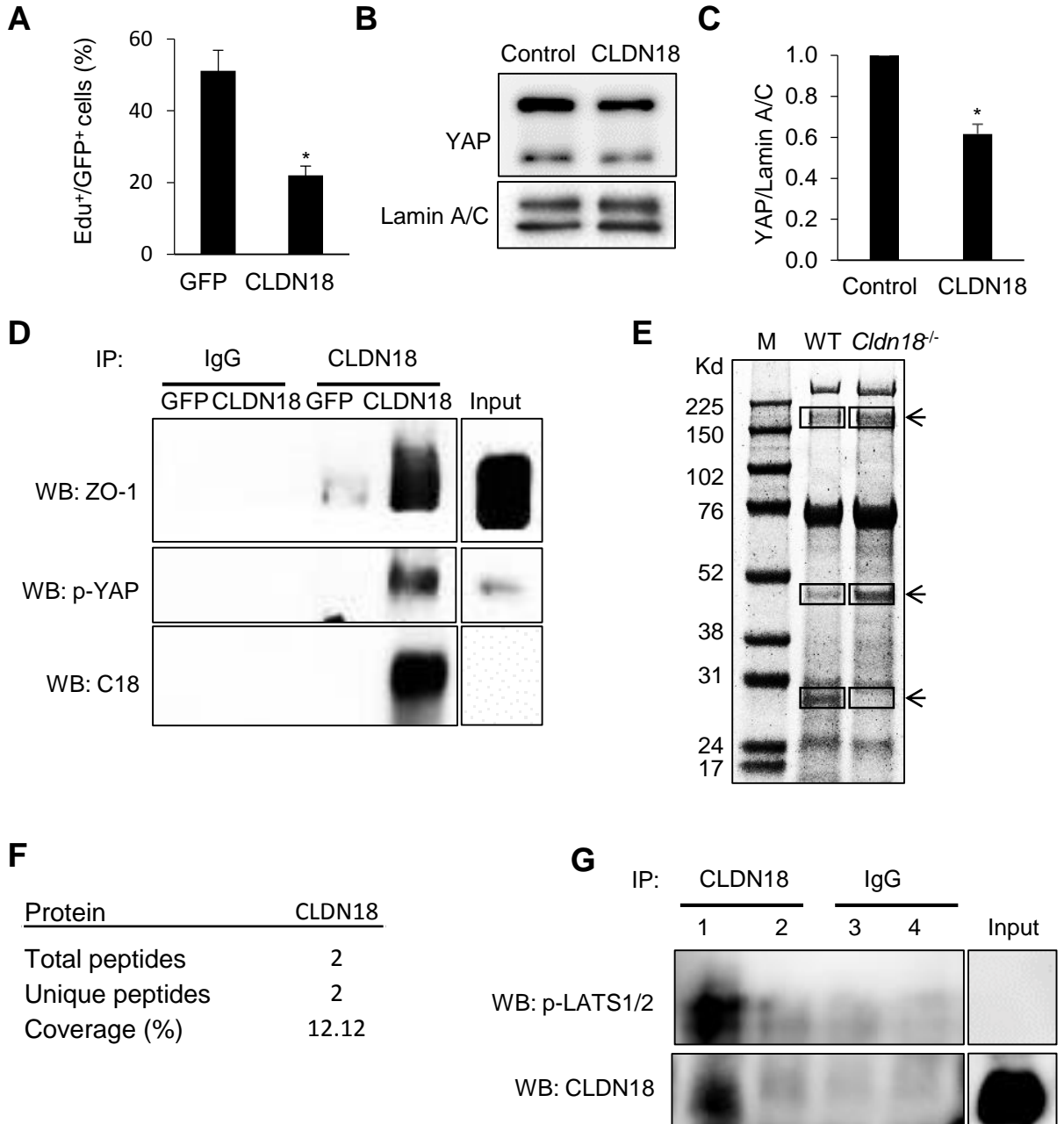
Supplemental Figure 11. Mixed 3D cultures of mT/mG (Tomato⁺) and unlabeled WT or *Cldn18*^{-/-} cells. Single sorted type II (AT2) cells from mT/mG mice and either WT or *Cldn18*^{-/-} mice were co-cultured with MLg fibroblasts in 3D Matrigel. Mixed cultures consisting of mT/mG and either WT or *Cldn18*^{-/-} cells formed colonies with either labeled or unlabeled cells, indicating clonality. Scale bar: 50 μ m.



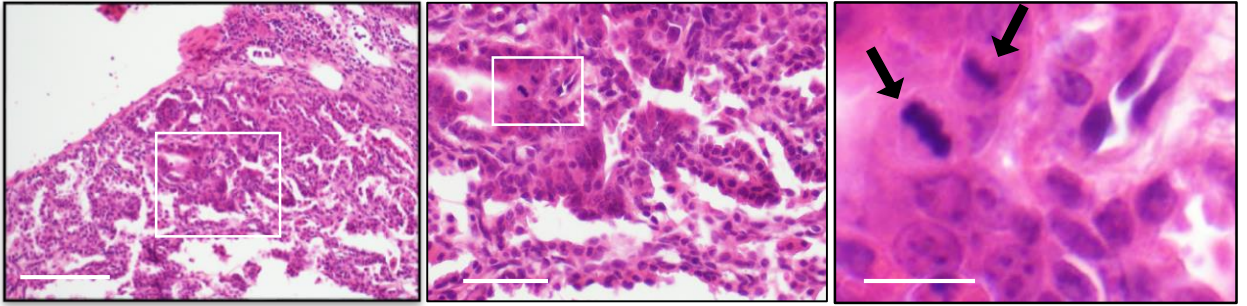
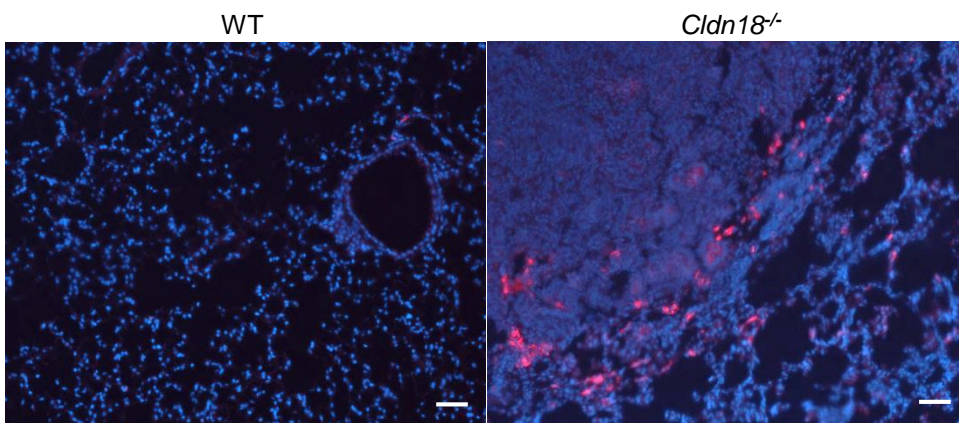
Supplemental Figure 12. Type II (AT2) to type I (AT1) cell transdifferentiation is similar in *Cldn18*^{-/-} and WT mice. AT2 cells isolated from WT and *Cldn18*^{-/-} mice were cultured on polycarbonate filters coated with laminin-5 for 6 days. Representative Western blot (**A**) shows a similar increase in AT1 cell markers T1α, AQP5 and RAGE during transdifferentiation from AT2 (Day 0) to AT1 cell-like phenotype (Day 6) in WT and *Cldn18*^{-/-} KO AT2 cells. (**B-D**) Two-Way ANOVA and linear regression analyses yielded no significant difference ($P>0.05$) of slopes for increase in AT1 cell markers over time between WT and *Cldn18* KO AT2 cell cultures. $n=3$.



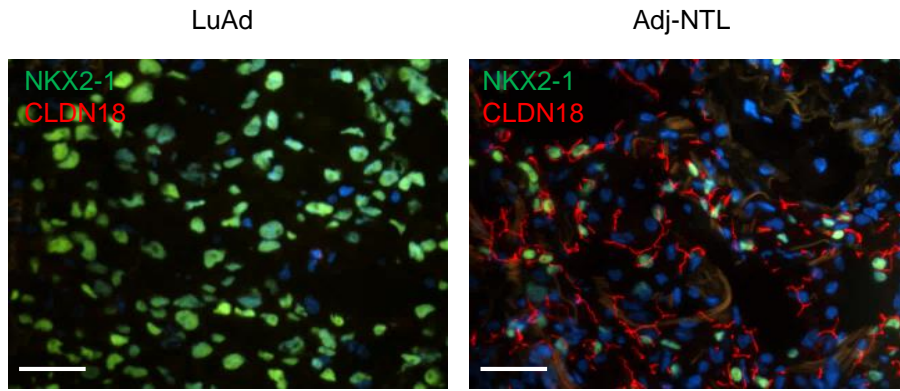
Supplemental Figure 13. Colony forming efficiency (CFE) following passage (P) of WT and *Cldn18*^{-/-} type II (AT2) cells. CFE remains increased in *Cldn18*^{-/-} compared to WT cells at P1. n=3. Z-test. *, vs. WT mice, $P < 0.05$. Bar graphs represent mean \pm SEM.



Supplemental Figure 14. CLDN18 regulates cell proliferation and YAP activity and interacts with p-YAP, p-LATS1/2 and ZO-1. CLDN18 overexpression in MLE-15 cells decreases proliferation (**A**) and nuclear YAP (**B** and **C**). $n \geq 3$ independent experiments. Unpaired 2-sided *t*-test for **A**, Z-test for **C**. *, $P < 0.05$. (**D**) Representative co-immunoprecipitation (co-IP) shows increased CLDN18 association with ZO-1 and p-YAP in MLE-15 cell membranes following CLDN18 overexpression. GFP is control vector. Input is cell lysate before IP as positive control; however, CLDN18 cannot be detected in input. $n=3$. (**E**) Lysates from WT and *Cldn18*^{-/-} AT2 cells were immunoprecipitated with anti-YAP antibody. Eluates were resolved by SDS-PAGE and highlighted Coomassie blue-stained bands (rectangle, arrow) were analyzed by mass spectrometry. (**F**) Mass spectrometry identified CLDN18 as a YAP-interacting protein in WT but not *Cldn18*^{-/-} lung. (**G**) IP of WT (1 and 3) and *Cldn18*^{-/-} (2 and 4) AT2 cell membrane lysates with anti-CLDN18 antibody shows endogenous CLDN18 associates with p-LATS1/2. IgG = negative control. Input is lung tissue lysate before IP as positive control; however, p-LATS1/2 cannot be detected in input. $n=2$. In **D** and **G**, input were run on the same gel but were non-contiguous.

A**B**

Supplemental Figure 15. Lung tumors in *Cldn18*^{-/-} mice. (A) Hematoxylin and eosin staining shows mitotic figures (arrows) in lung tumor in *Cldn18*^{-/-} mice. From left to right, bars = 400 μ m, 100 μ m and 40 μ m. (B) Immunofluorescence of lung tissue shows tumor infiltration with CD68⁺ macrophages (red). DAPI (blue) is the nuclear counterstain. Scale bar: 50 μ m.



Supplemental Figure 16. Double labeling for CLDN18 and NKX2-1 in lung tumors. Immunofluorescence shows decreased CLDN18 protein expression in human LuAd compared to adjacent non-tumor lung (Adj-NTL). n=3. Scale bar: 50 μ m. DAPI is the nuclear counterstain.

Supplemental Table 1. Summary of volume measurement of WT and *Cldn18*^{-/-} lungs by micro-CT

Measurement	WT1	WT2	WT3	WT Average	<i>Cldn18</i> ^{-/-} 1	<i>Cldn18</i> ^{-/-} 2	<i>Cldn18</i> ^{-/-} 3	<i>Cldn18</i> ^{-/-} Average
Total lung (V_{Tlung}, cm³)	0.644	0.591	0.613	0.616	1.166	1.022	0.966	1.051*
• Conducting airway ($V_{Cairway}$, cm³)	0.110	0.100	0.106	0.105	0.153	0.125	0.114	0.131
• Alveolar airspace (V_{alv}, cm³)	0.424	0.393	0.397	0.404	0.362	0.363	0.370	0.365
❖ Volume fraction of alveolar airspace in alveoli (F_{alv})	0.790	0.790	0.780	0.790	0.360	0.400	0.430	0.400
• Parenchyma (V_{par}, cm³)	0.111	0.098	0.110	0.106	0.651	0.534	0.483	0.556*
❖ Volume fraction of parenchyma in alveoli (F_{par})	0.210	0.210	0.220	0.210	0.640	0.600	0.570	0.600

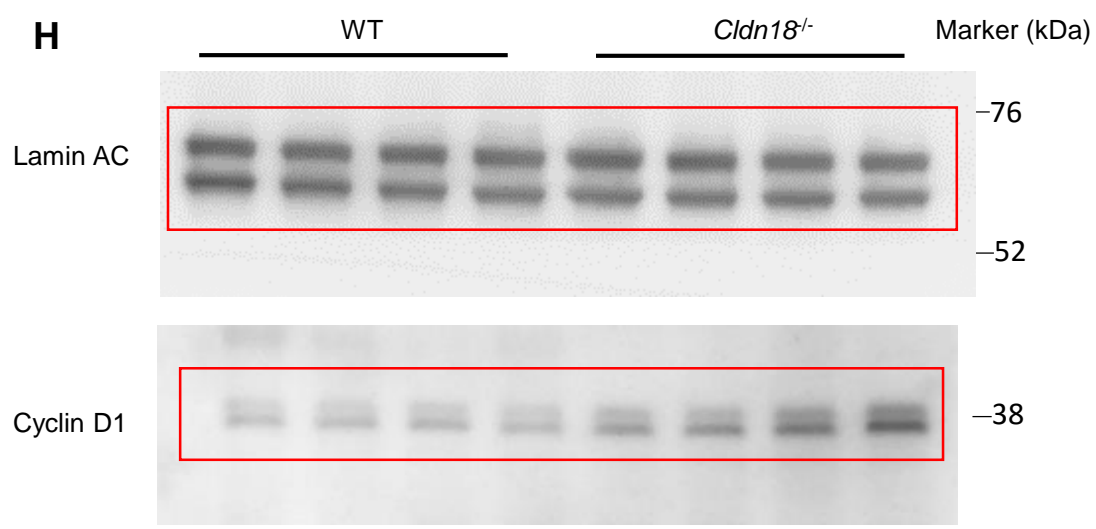
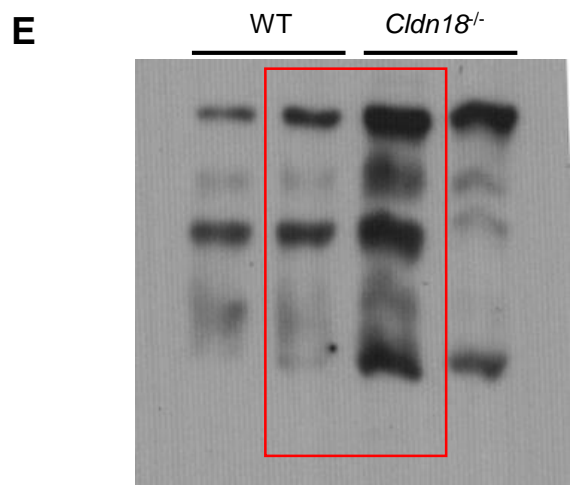
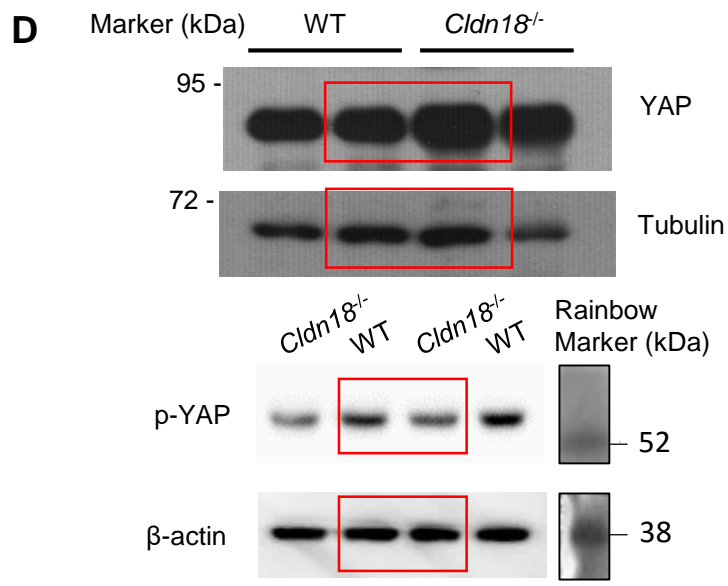
n = 3. Unpaired 2-tailed t-test. *, $P < 0.05$ compared to WT.

Supplemental Table 2. Tumor number and volume in aged *Cldn18^{-/-}* mice

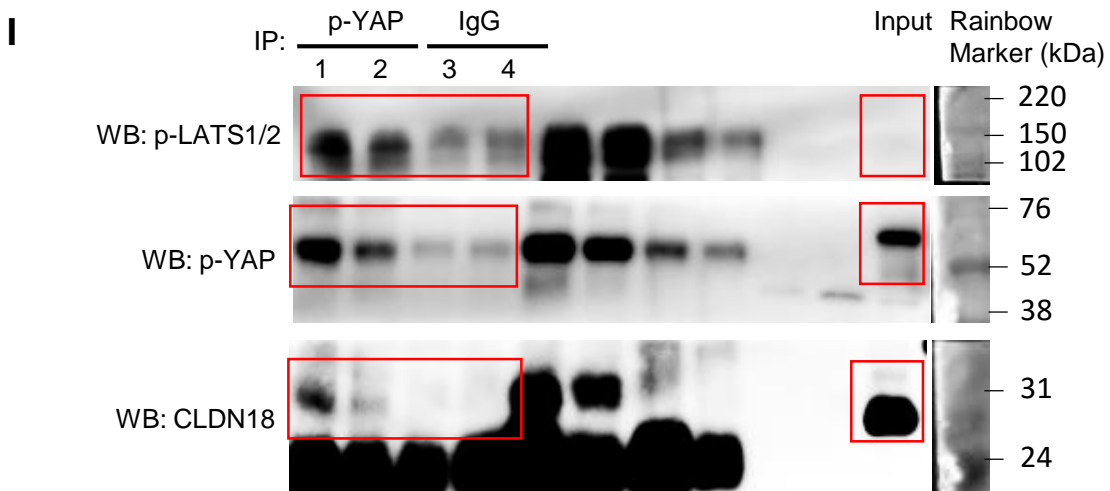
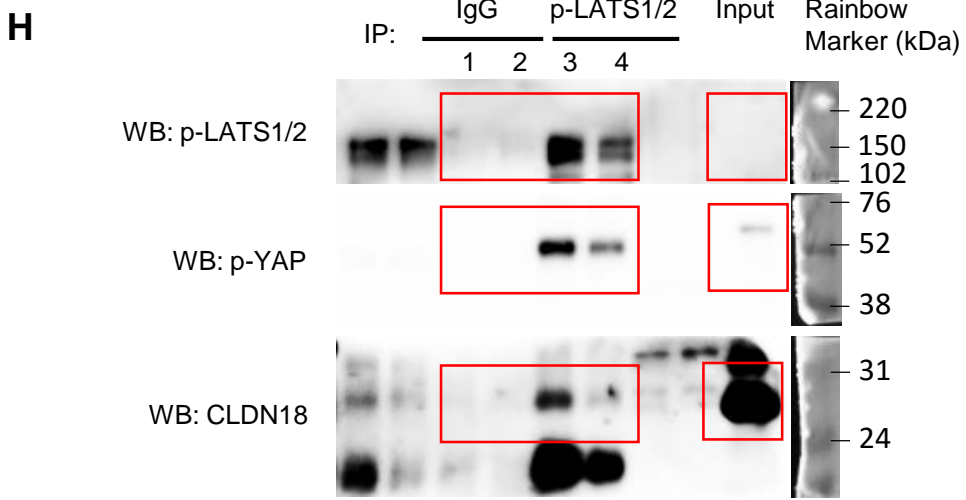
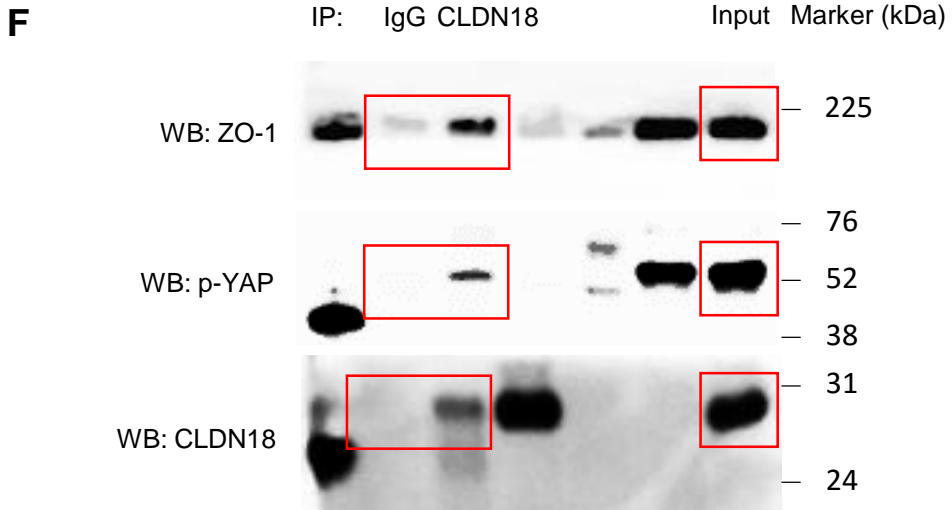
Mice	Tumor number	Tumor volume (V, mm³)
Cldn18^{-/-} 1	3	1.21
		0.61
		0.35
Cldn18^{-/-} 2	2	29.6
		9.34
Cldn18^{-/-} 3	4	6.48
		2.4
		2.1
		2
WT1	0	—
WT2	0	—
WT3	0	—

Full unedited gels for **Figures and Supplemental Figures**

Full unedited gels for Figure 3

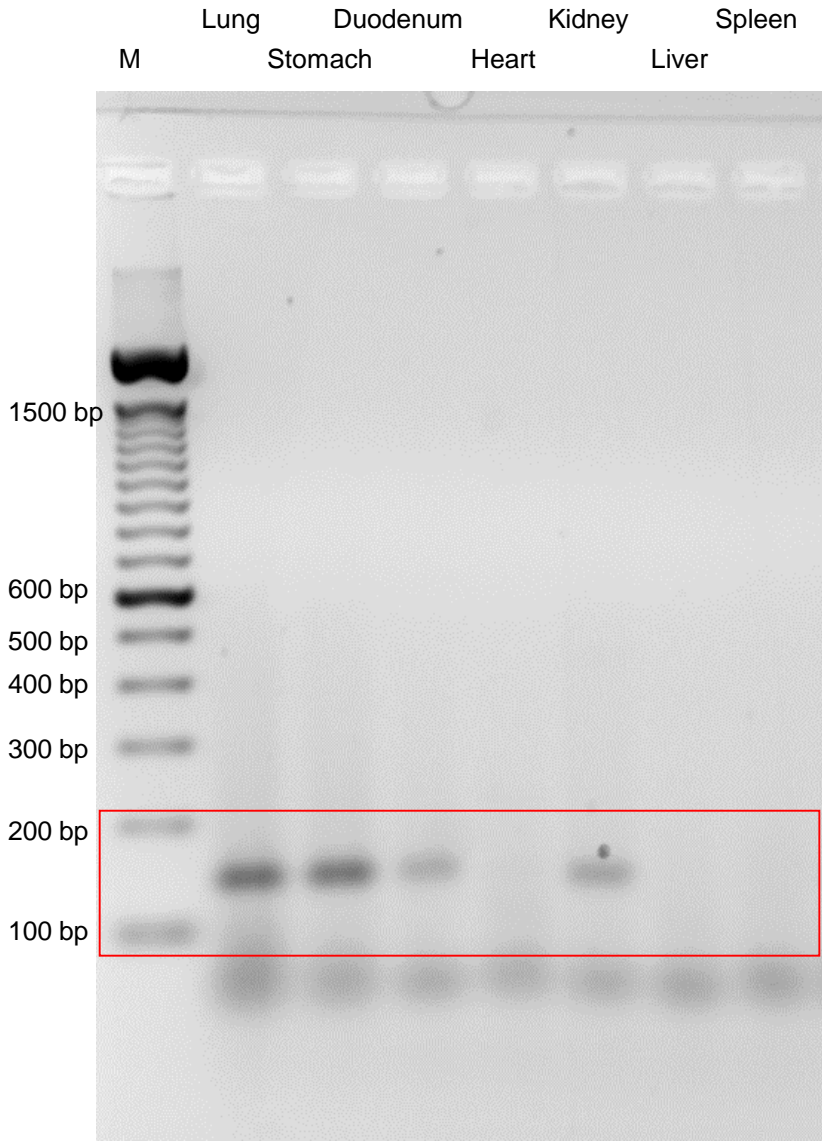


Full unedited gels for **Figure 5**

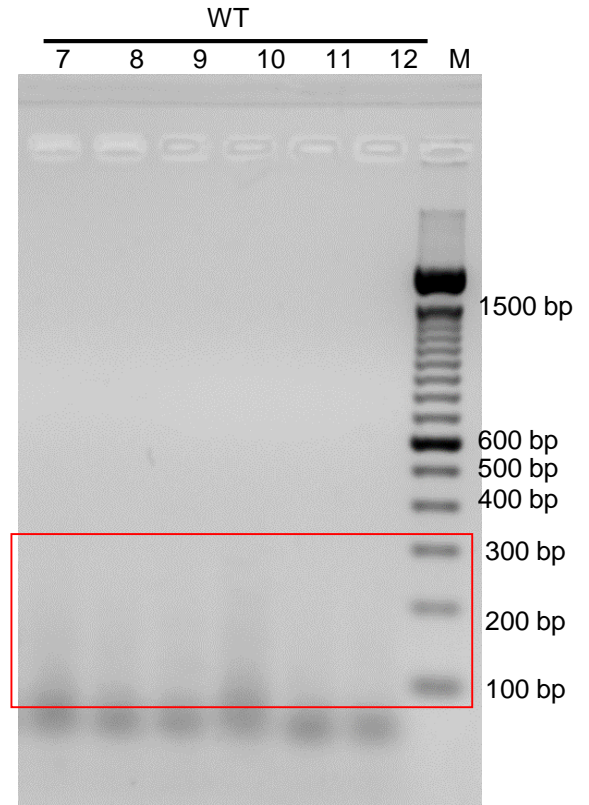
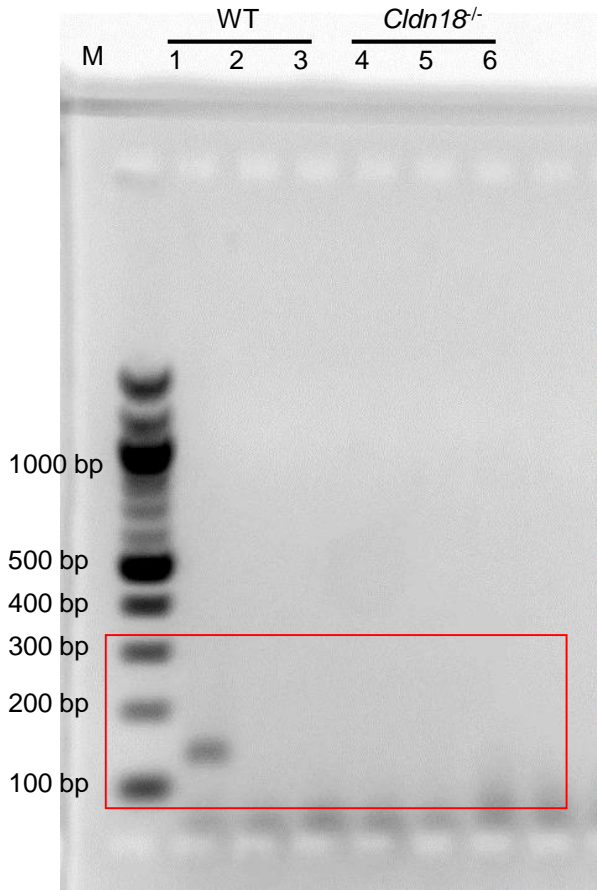


Full unedited gels for **Supplemental Figure 3**

A

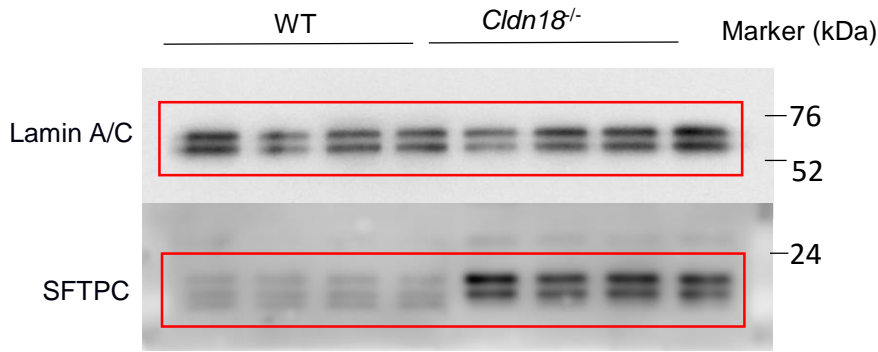


D

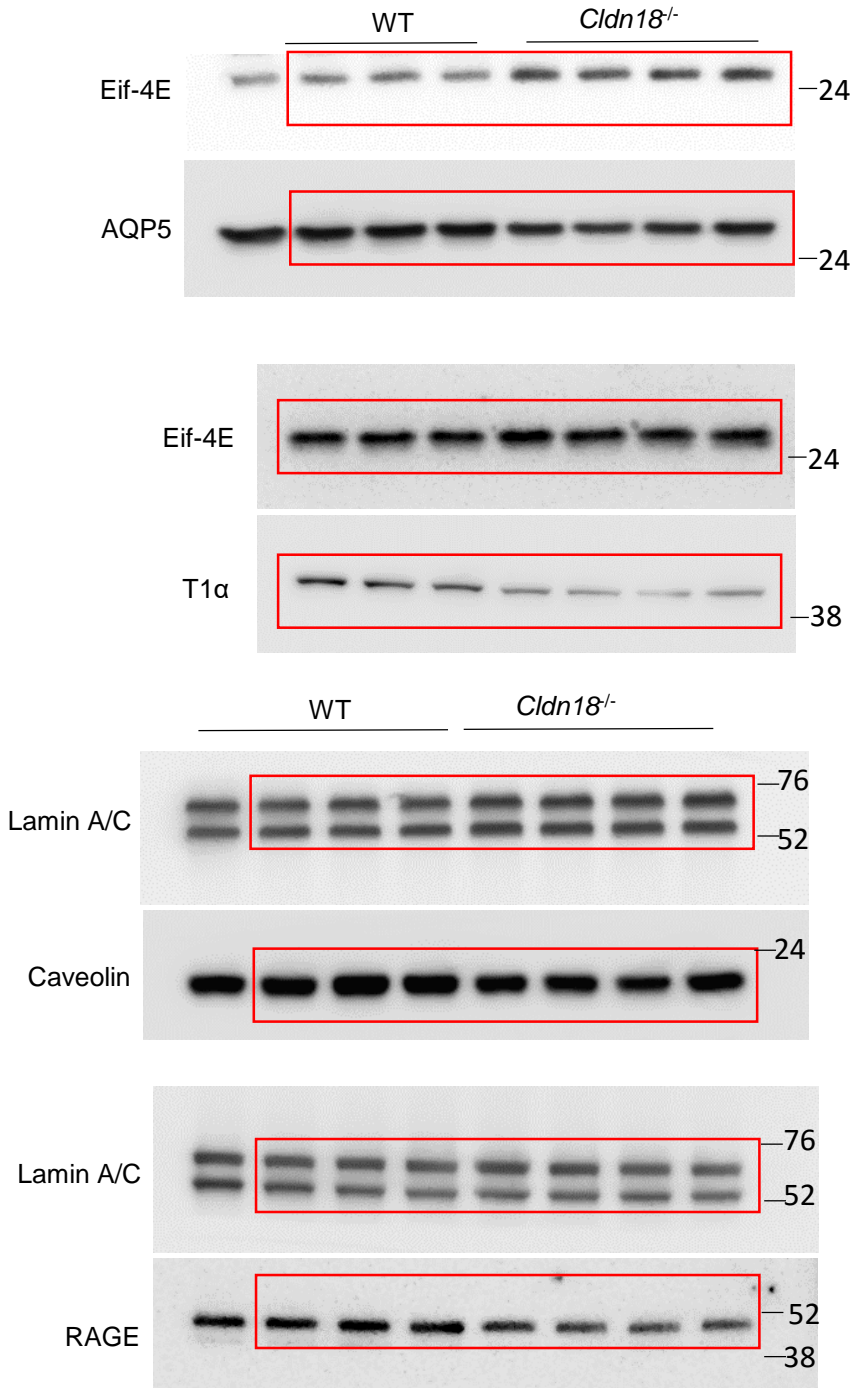


Full unedited gels for Supplemental Figure 6

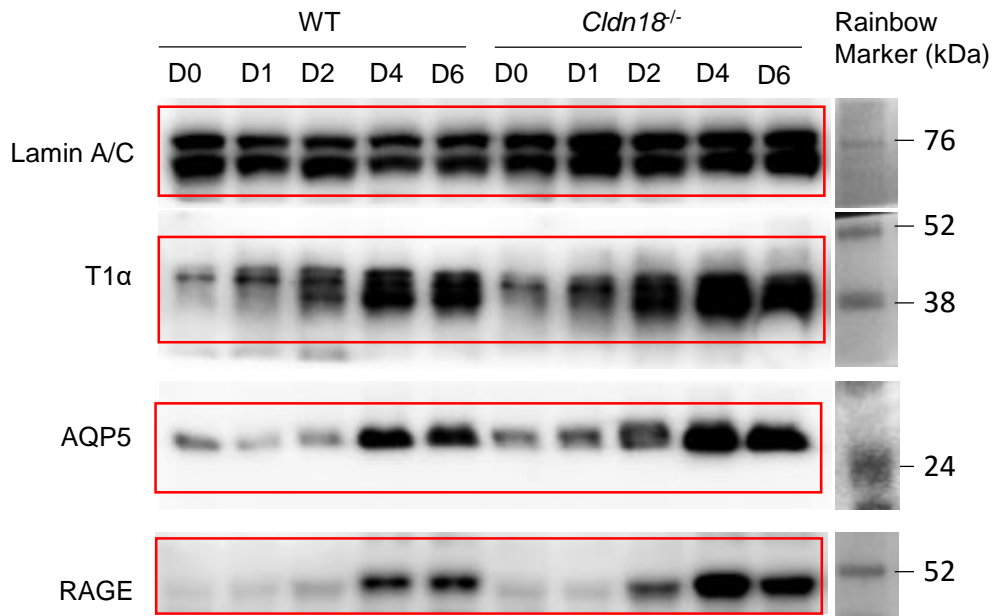
A



C

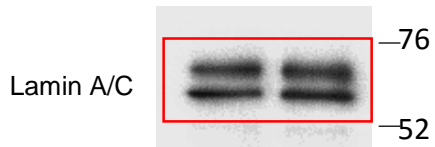
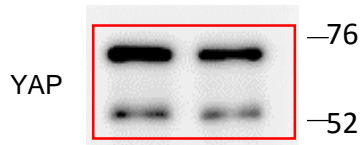


Full unedited gels for **Supplemental Figure 12**

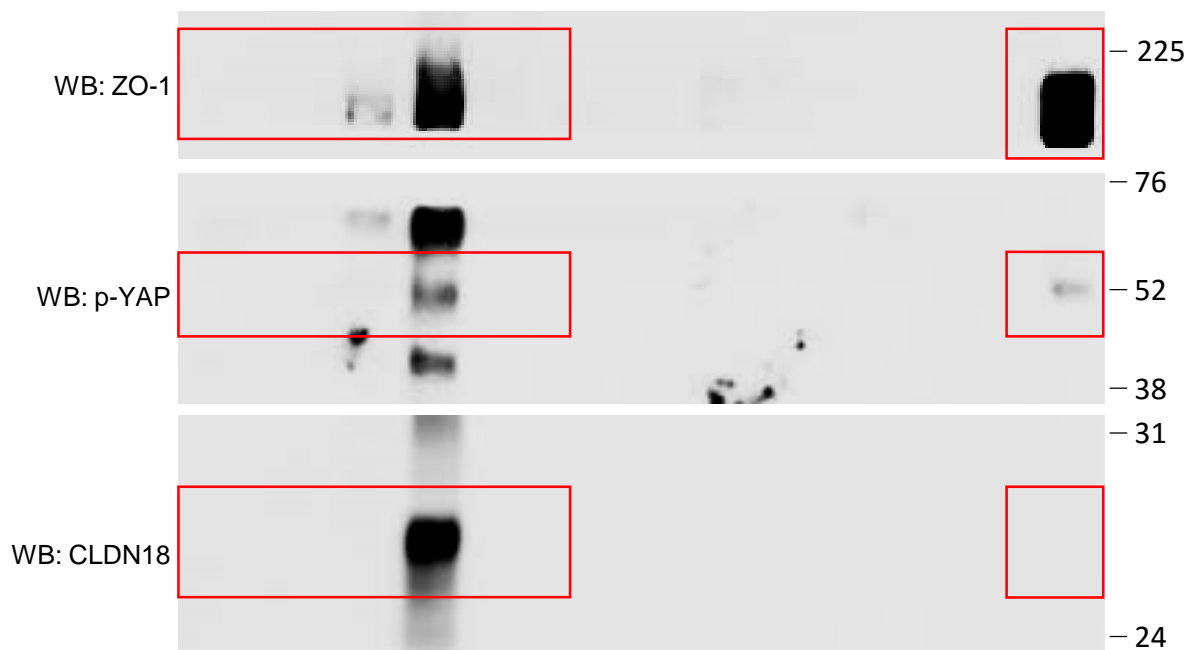


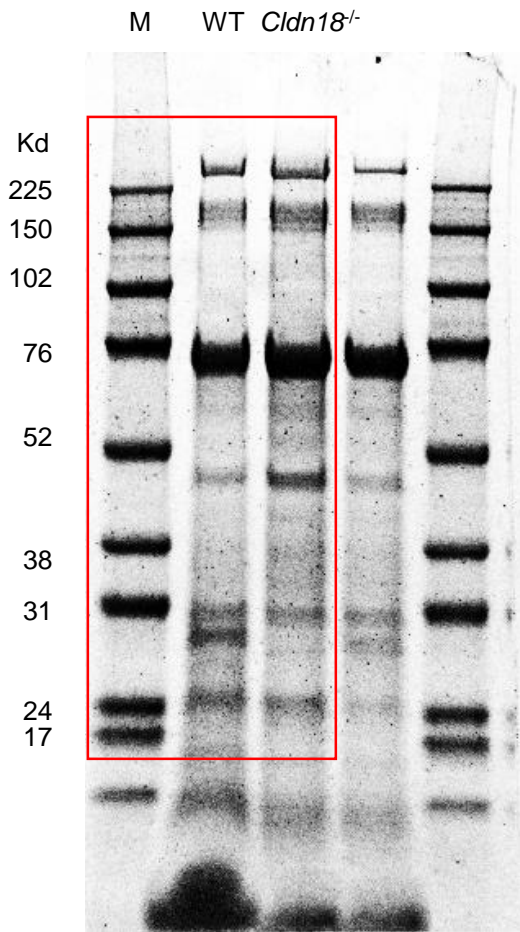
Full unedited gels for Supplemental Figure 14

B Control CLDN18 Marker (kDa)



D IP: IgG CLDN18 Input Marker (kDa)
GFP CLDN18 GFP CLDN18



E**G**